THE PRESENT-DAY STRESS FIELD PATTERN IN THE EASTERN CARPATHIAN BEND AREA

GABRIELA POLONIC, DOREL ZUGRĂVESCU, VICTOR NEGOIȚĂ

"Sabba S. Ştefănescu" Institute of Geodynamics of the Romanian Academy
19–21 Jean-Louis Calderon St., 020032, Bucharest 37, Romania

Le modèle du stress actuel dans la zone de Courbure des Carpates Orientales. L'étude présente une analyse détaillée des champs de stress actuel, pour la zone de Courbure des Carpates Orientales, en vue de définir le modèle caractéristique, avec des implications dans la dynamique récente des compartiments crustaux. Les données ont été obtenues par deux méthodes: une méthode directe, basée sur l'analyse des ovalisations du trou de forage enregistrées par les diagraphies SHDT et Diplog (37 données), pour définir la contrainte horizontale maximale dans la partie supérieure de la couverture sédimentaire, et une méthode inverse, basée sur l'étude des mécanismes en foyer des séismes croûtaux (72 données) pour définir les orientations des principaux axes de stress σ_1, σ_2, σ_3, dans l'entière épaisseur de la croûte. Le champ de stress actuel a un caractère homogène, compressive, exprimé par une orientation spatiale prédominante NO-SE de la contrainte horizontale maximale dans la Microplaque Mœsienne, avec une rotation dextre des plans d'environ 30°, entre le Promontoire Nord-Dobrogéen et le Bloc Central de la Plate-forme Mœsienne. L'étude a prouvé une variation du champ de stress actuel en profondeur, en ce qui concerne: le changement de l'orientation de la contrainte horizontale maximale, en rotation dextre à partir de la couverture sédimentaire (105°), vers la limite avec le soubassement cristallin (125°), et la discontinuité Conrad (135°), jusqu'à la partie inférieure de la croûte (150°); le changement du régime tectonique, déterminé par l'augmentation du stress horizontal dans la partie supérieure de la croûte, à cause de la collision continentale des compartiments crustaux qui est exprimé par un régime prédominant compressif, de décrochement horizontal jusqu'au niveau du soubassement cristallin et inverse jusqu'à la discontinuité Conrad. La présence du stress vertical dans la partie inférieure de la croûte, à cause de l'augmentation de la pesanteur par surcharge, est matérialisée par un régime extensif.

Key words: present-day stress field, breakouts and earthquakes focal mechanism, Carpathian bend area, Vrancea.

1. INTRODUCTION

It is well known that the intra-plate tectonic stress field can be used to determine the direction and relative magnitude of the various forces controlling the plate motion and to provide data for assessing the origin of tectonic movements and seismicity. The causal connection between the tectonic phenomenon, *i.e.*, the faulting and the three main stress directions in the Earth's crust, grounded as far back as the beginning of the fifties (Anderson, 1951), consists in the fact that in the areas of deviatoric extension (normal faulting) the maximum principal stress is vertical, in areas of deviatoric compression (thrust fault) the minimum principal stress is vertical and in areas of strike-slip faulting the vertical stress is an intermediate one. Seismological studies lead to the conclusion that most of the earthquakes are the consequence of such faulting, which has taken place somewhere in the brittle regions of the crust.

In 1996, the Institute of Geodynamics initiated detailed and systematic studies regarding the present-day stress field determination, in order to complete the image of the lithosphere compartments recent dynamics. The investigations aimed at the determination of the present-day stress field parameters, among which the maximum stress tensor orientation reflects the force direction acting on the respective compartment.

Two methods were used to obtain stress orientations:

– a direct one, based on the analysis of the stress-induced well bore enlargements, „the breakouts“ produced during the drilling (Zugrăvescu *et al.*, 1998, 2000 a, b, 2002) and

– an inverse method, based on the study of the earthquake focal mechanisms (Zugrăvescu, Polonic, 1997, 2000, 2003).

In Romania, studies regarding the maximum stress orientation, based only on the well logging method, were published previously by Neguț *et al.* (1994, 2000), offering scarce and nonuniform information.

This study intends to offer a detailed analysis of the stress data obtained by the combination of the two methods, presented till now only separated, to point out the variation of the stress data with depth and finally to draw the pattern of the present-day stress field in the Eastern Carpathian bend area with its implication in the recent dynamics.

2. STRUCTURAL SETTING

The study is focused on the bending area of the Eastern Carpathians, especially on the Carpathian foreland, composed of the south-western segment of the East-European Platform (EEP), the north-eastern part of the Moesian Platform (MP), as well as the remains of an Early Alpine Orogen in-between, the North Dobruja Orogen (NDO) with its north-western prolongation, the North-Dobrujan Promontory (NDP).

This area corresponds to the biggest width of the East Carpathian Orogen overthrust on the foreland platforms. The Eastern Carpathians, composed of the well known structural units (Săndulescu, 1984, 1988), resulted from the two main compressional events which took place during the Cretaceous, with the accretion of the Dacidic units and during the Neogene, with the accretion of the Moldavides units and the transport of the structural complex to the present position

(Săndulescu, 1988). The newest tectonic event, corresponding to the Wallachian phase (1.60–1.0 My), generated foldings and overlapping with reduced horizontal displacement in the Subcarpathian nappe cover and the internal part of the foredeep, limited by the Intra-Moesian (IM) and Peceneaga–Camena (PC) faults.

The outer foredeep represents an asymmetric depression, with the typical development in the "Focşani Depression", its major part being superimposed on the foreland.

More detailed data concerning the Orogen structure are presented by Săndulescu (1984, 1988), Săndulescu, Visarion (2000) and concerning the foreland units, from the oil drilling activity results interpretation (Paraschiv, 1979; Ionesi, 1994 and Tărăpoancă *et al.*, 2003).

The deep crustal structure in the bending area of the Eastern Carpathians reflects the convergence processes of the lithospheric compartments, the European Plate and other Microplates (Intra-Carpathians and Moesian) partially welded at the southern margin. Its complexity was emphasized by the crossing refraction seismic profiles: XI – Oradea–Galați; XI_1 – Focşani–Jirlău; II – Călăraşi–Galați (Rădulescu *et al.*, 1976), Bacău–Giurgiu (Hauser *et al.*, 2001), Oradea–Black Sea (Landes *et al.*, 2004).

Structural maps drawn at the three main discontinuities such as the crystalline basement level (Polonic, 1996, 1998, 2002), the Conrad and Moho discontinuities (Rădulescu, 1988), offered suggestive images of the deep crustal structure.

An important consequence of the convergence processes from the Eastern Carpathian bend area is the presence of the seismic Vrancea region, characterized by a narrow vertical elongated intermediate seismicity source zone (40 × 80 km width, h = 60–180 km), with large earthquakes (Mw ≤ 7.4) and a widely spread crustal seismicity zone, with moderate magnitudes events (Mw ≤ 5.6, h = 10–40 km), a weak seismic zone, located between 40–60 km, separating the two above mentioned source zones (Constantinescu and Mârza, 1980; Oncescu *et al.*, 1999).

3. THE PRESENT-DAY STRESS FIELD INFERRED FROM THE BREAKOUTS METHOD

3.1. METHODOLOGY

We shall begin with the presentation of the stress field characteristics from surface to depth, using the data from the upper part of the sedimentary cover, up to the depth of 5 km, obtained from the boreholes.

Well bore breakouts, the preferential elongation of the borehole cross-section over a great depth interval, resulted from shear fracturing in the region of maximum compressive stress, were used in the determination of the recent stress during the last 4 years, by the Institute of Geodynamics of the Romanian Academy. The studies tried to ascertain in the Carpathian bend area the azimuths of the horizontal component orientations of the maximum (S_{Hmax}) and minimum (S_{hmin}) stresses.

In the Carpathian bend area, the field data of this work proceed from the well logging operations performed during the last 10 years with Schlumberger and

Western equipments. Most of these measurements for stress orientation, based on the breakout method, were carried out using the Schlumberger 4 arms SHDT device (Stratigraphic High Resolution Diameter Tool) and the Western Diplog, without any complementary information coming from the Borehole Televiewer or the Formation Microscanner.

In the study area, our observations of gauge hole sand layers and elongated borehole geometry of neighbouring shales are consistent with borehole stability and rock mechanical properties. These observations pointed out compressive shear failure of shale rock intervals and consequently a hole enlargement in the direction of the minimum horizontal stress component.

In our stress studies we used the liniar isotropic poroelastic stress-strain theory, considering the strain plane orthogonal to the borehole axis. The elipsoid of stress was defined by giving the direction of its three orthogonal axes and the corresponding stress magnitude values S_1, S_2, S_3, known as the principal stresses.

3.2. DATA

In the bending area of the Carpathians, 37 determinations of the stress data, resulted from the breakout measurements in the boreholes, according to the WSM ranking system (Zoback, 1992; Müller, 1993) were selected (Table 1). They are registered in the stress data files together with the following data: the age and the lithology of the deposits, the geological structure, the registered intervals with distinct borehole breakouts, the total length of the investigated breakouts, the horizontal component orientations of the maximum (S_{Hmax}) and minimum stress (S_{Hmin}) as well as the quality rank of the determinations according to the WSM indications.

The data present a good confidence degree: 5.3% for the A rank, 44.7% for the B rank and 50% for the C rank. If we consider the depth distribution of borehole data with respect to the quality, we observe that the A rank data are situated between 1.5–2 km, the B and C ranks data are concentrated at the depth between 1.2–3.5 km. A great number of data come from a depth of 1–3 km, under which they are drastically reduced.

The azimuths of the maximum horizontal stress component were plotted on the structural map of the Eastern Carpathians bending area (Fig. 1). The investigated deposits, between 200–5,000 m, were Mesozoic, Paleogene and Miocene in age, belonging to the Tarcău, Marginal folds or Subcarpathian Nappes and of Miocene–Pliocene age, belonging to the foredeep or to the Moesian Platform cover.

On the inner flank of the foredeep, the borehole measurements were performed in the Upper Miocene–Pliocene deposits of the diapir-salt zone, one of the most prolific area for oil accumulation. In this area, the structures, disposed along the longitudinal regional faults, on at least five alignments, are characterized by different salt piercing features, which gave successively, towards the outer part, different kind of diapirs: overflowed, exaggerated, attenuated or cryptodiapirs.

Table 1

Stress data determined by breakout measurements

Crt. no.	Geological structure/ District	Geological format. Age	Lithology	Registered interval (m)	Breakout lengths (m)	$S_{H\,max}$ (°)	$S_{h\,min}$ (°)	Geol. unity	Quality rank	Symbol on the map
1	2	3	4	5	6	7	8	9	10	11
1	Amaru (Buzău)	Sm	c, si, s, st	4387-2097	171	96	06	MP	B	A
2	Băicoi (Prahova)	Pn/Me/Sm	C, si, s, st	2665-287	260	63	153	Fdp	B	Bă
3	Bărbuncești 1 (Buzău)	Me	C, si, s	2727-2530	100	122	32	Fdp.	C	Bb
4	Bărbuncești 2 (Buzău)	Me	C, si, s, st	2952-2550	229	167	77	Fdp,	C	Bb
5	Bărbuncești 3 (Buzău)	Me	C, si, s, st	2656-2428	118	143	53	Fdp.	B	Bb
6	Berca 1 (Buzău)	Pn/Me	C, si, s, st	1753-747	426	138	48	Fdp.	B	Be
7	Berca 2 (Buzău)	Pn/Me	C, si, s, st	1164-199	284	128	38	Fdp.	B	Be
8	Berca 3 (Buzău)	Pn/Me	C, si, s, st	1324-348	393	122	32	Fdp.	B	Be
9	Bobocu (Buzău)	Dc/Pn	S, si, c	2627-1186	140	118	38	MP	B	Bu
10	Boldești 1 (Prahova)	Pn/Me/Sm	C, si, s, st	2318-1483	334	135	45	Fdp.	B	Bo
11	Boldești 2 (Prahova)	Dc/Pn/Me	S, st, si, c	2243-1573	270	128	38	Fdp.	B	Bo
12	Buda (Vrancea)	Pl/Sm	C, si, s, st	2949-996	470	86	176	NDP	B	Bd
13	Burloiu-Buștenari (Prahova)	Ol	c, s, st	1946-301	520	53	143	Fdp	B	Br
14	Cărbunești (Prahova)	Pn/Me/Hv /Ol	c, s, si, st	900-205	138	58	148	Fdp	B	C
15	Cioceni (Prahova)	Dc/Pn	C, s, st	2500-2000	31	109	19	MP	C	Ci
16	Colibași (Dâmbovița)	Ol	S, st, c	2451-1484	450	35	125	Fdp	C	Cl
17	Conduratu (Prahova)	Pn/Me/Sm	C, s, si, st	3898-2698	520	98	08	MP	B	Co
18	Drăgăești/(Dâmbovița)	Me/Sm/Hv	S, c, st	1702-750	547	28	118	Fdp	A	D
19	Independența (Galați)	Pl/Sm	S, c	1005-195	210	116	26	DP	C	I
20	Lipia (Ilfov)	Dc/Pn/Me	C, si, s	1742-495	306	85	175	MP	B	L
21	Măgurele 1 (Prahova)	Pn/Me/Hv	C, si, s, st	2233-1982	115	55	145	Fdp	C	M
22	Măgurele 2 (Prahova)	Hv	St, s, c	2355-2235	55	60	150	Fdp	C	M
23	Monteoru (Buzău)	Pn/Me	C, si, s	1003 - 208	237	109	19	Fdp	B	Mo

(*continues*)

Table 1 (continued)

1	2	3	4	5	6	7	8	9	10	11
24	Nineasa (Bacău)	Ol.	C, s, st	1008 - 741	32	108	18	Mdv	C	Ni
25	Ochiuri 1 (Dâmbovița)	Dc/Pn/Me	S, st, c	1175-1000	65	120	30	Fdp	C	O
26	Ochiuri 2 (Dâmbovița)	Pn/Me/Hv	S, st, si, c	1401-1191	133	102	12	Fdp	C	O
27	Ochiuri 3 (Dâmbovița)	Pn/Me/Hv	S, st, si, c	1351-1000	84	25	115	Fdp	C	O
28	Ocnița (Dâmbovița)	Dc/Pn/Me/ Hv/Ol	S, st, si, c	1804 - 400	620	41	131	Fdp	C	Oc
29	Păcureți (Prahova)	Pn/Me	C, si, st, s	1400 - 280	525	54	144	Fdp	A	P
30	Poiana Sărată (Bacău)	Mi/Ol/Eo	C, s, st, si	1599 - 955	320	136	46	Mdv	B	PS
31	Roșiori (Buzău)	Dc/Pn	C, s, st, si	2502-1202	115	106	16	MP	B	R
32	Runcu (Prahova)	Hv/Ol	C, s, st	2047 - 600	76	168	78	Fdp	C	Ru
33	Sibiciu (Buzău)	Ol	C, st	4883-4000	178	30	120	Mdv	C	Sb
34	Șirna (Prahova)	Bd/Eo/Cr	Ç, st	4143-3615	48	92	02	MP	C	Și
35	Urziceni (Ialomița)	Me	C, si, st	1227 - 300	41	110	20	MP	C	U
36	Vintileanca (Buzău)	Dc/Pn/Me/ Sm	C, si, s, st	3802 - 999	550	82	172	Fdp	C	V
37	Vlădeni (Prahova)	Dc	C, si, s	1297 - 300	40	81	171	MP	C	Vl

Age of the geological formations: Pl – Pliocene; Dc – Dacian; Pn – Pontian; Me – Meotian; Mi – Miocene; Sm – Sarmatian; Bd – Badenian; Hv – Helvetian; Ol – Oligocene; Eo – Eocene; Cr – Cretaceous.

Lithology: c – clay; si – silt; s – sand; st – sandstone.

Geological unity: Mdv – Moldavides; Fdp – Foredeep; MP – Moesian Platform; NDP – North Dobruja Promontory.

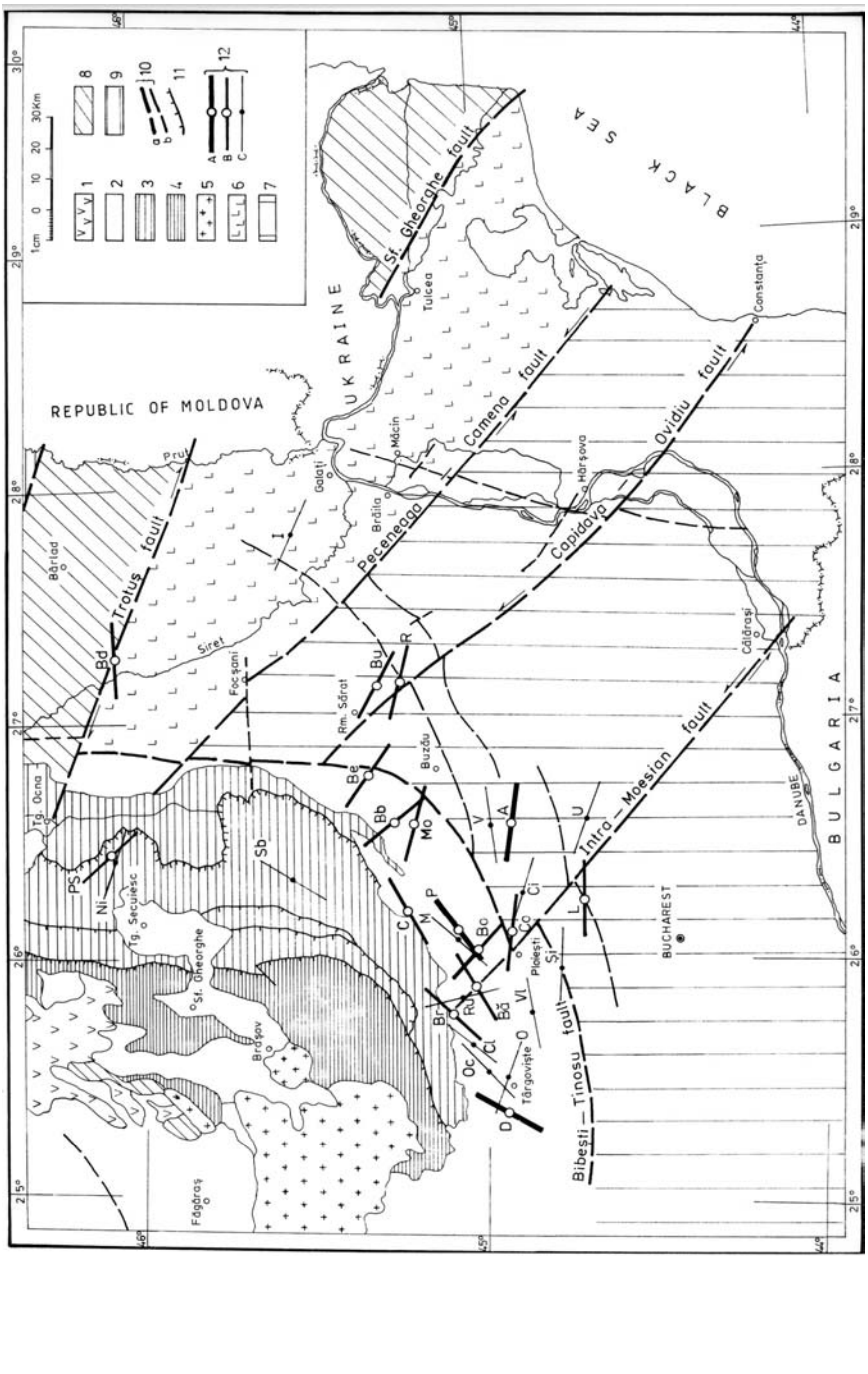

Fig. 1 – Distribution of the borehole stress data (S_{Hmax}) on the structural map of the Carpathian bend area. 1, Neogene volcanites; 2, Foredeep and molassic depressions; 3, Moldavides; 4, Outer Dacides; 5, Median Dacides; 6, North Dobrujan Promontory; 7, Moesian Platform; 8, Scythian Platform; 9, European Platform; 10**a**, crustal fault; **b**, fault; 11, overthrusting line; 12, orientations of the borehole stress data, with the rank quality specification (A, B, C).

Two main regimes of the principal horizontal azimuths can be distinguished: a NW–SE regime, specific for the northeastern part of the Moesian Microplate and a NE–SW one for the western part of this unit.

The NW–SE stress regime is related, mainly, to the inner and outer flank of the foredeep, to the Moesian Platform cover and to the North Dobruja Promontory.

On the inner flank of the foredeep, the data set is coming from the wells carried out in the oil structures: Berca (Be), Bărbunceşti (Bb), Monteoru (Mo), Boldeşti (Bo), Runcu (Ru), the azimuths of the main horizontal stress varying from 120 to168° (Table 1, Fig. 1).

The Upper Miocene-Pliocene deposits, belonging to the outer flank of the foredeep, disposed on the foreland units, as well as those belonging to the Moesian Platform cover, were investigated in the Bobocu (Bu), Roşiori (R), Vintileanca (V), Amaru (A), Cioceni (Ci), Conduratu (Co), Urziceni (U), Lipia (L), Şirna (Şi) and Vlădeni (Vl) structures, the main stress horizontal azimuth varying from 80 to116° (Table 1, Fig.1).

The NW-SE stress regime is specific for the structures related to the platform basement and is due to the compression acting from the SE.

The NE-SW stress regime. In the proximity of the Intra-Moesian fault (IM fault), the azimuths of the maximum horizontal stress display a prevailing NE–SW orientation. The measurements of the borehole breakouts were performed in the Carpathian Orogene formations, involved in the Tarcău nappe (Sibiciu–Si structure) but, mainly, in the inner flank of the foredeep, the diapir salt zone, west and east from the IM fault, in the Miocene–Pliocene formations from the oil structures: Drăgăeşti (D), Ocniţa (O), Colibaşi (Cl), Burloiu (Br), Băicoi (Bă), Cărbuneşti (C), Măgurele (M) and Păcureţi (P), where orientations of 40–60º of the maximum horizontal stress orientations were determined (Table 1, Fig. 1).

Data analysis was performed by carrying out the frequency/rose diagrams on the basis of the maximum horizontal stress tensor orientations, for each compartment. For the *North Dobruja Promontory*, although the data are scared, a WNW–ESE orientation is detected (II_1, Fig. 2).

In the *north-eastern sector of the Moesian Platform* ($III_{1\text{-}2}$, Fig. 2), the 23 data outline a frequency diagram which displays two main trends: a prevalent WNW–ESE azimuth, corresponding to the orientation of the present-day compressions and displacements and a NE–SW one, parallel to the front of Carpathian Orogen.

In the *Central Block of the Moesian Platform* and in the vicinity of the Intra-Moesian fault ($III_{3\text{-}4}$, Fig. 2), the 9 azimuth determinations of the maximum horizontal stress display a bimodal general orientation: an almost E–W direction, which corresponds to the present-day compressions and a NE–SW second one, for the structures from the diapir salt zone, which can be assigned to the deviatory effect of the IMF and to these structures influence. The frequent modifications of the horizontal stress orientations can be observed in the diapir-salt structures, in the vicinity of the IM fault, from Drăgăeşti (D) to Cărbuneşti (C).

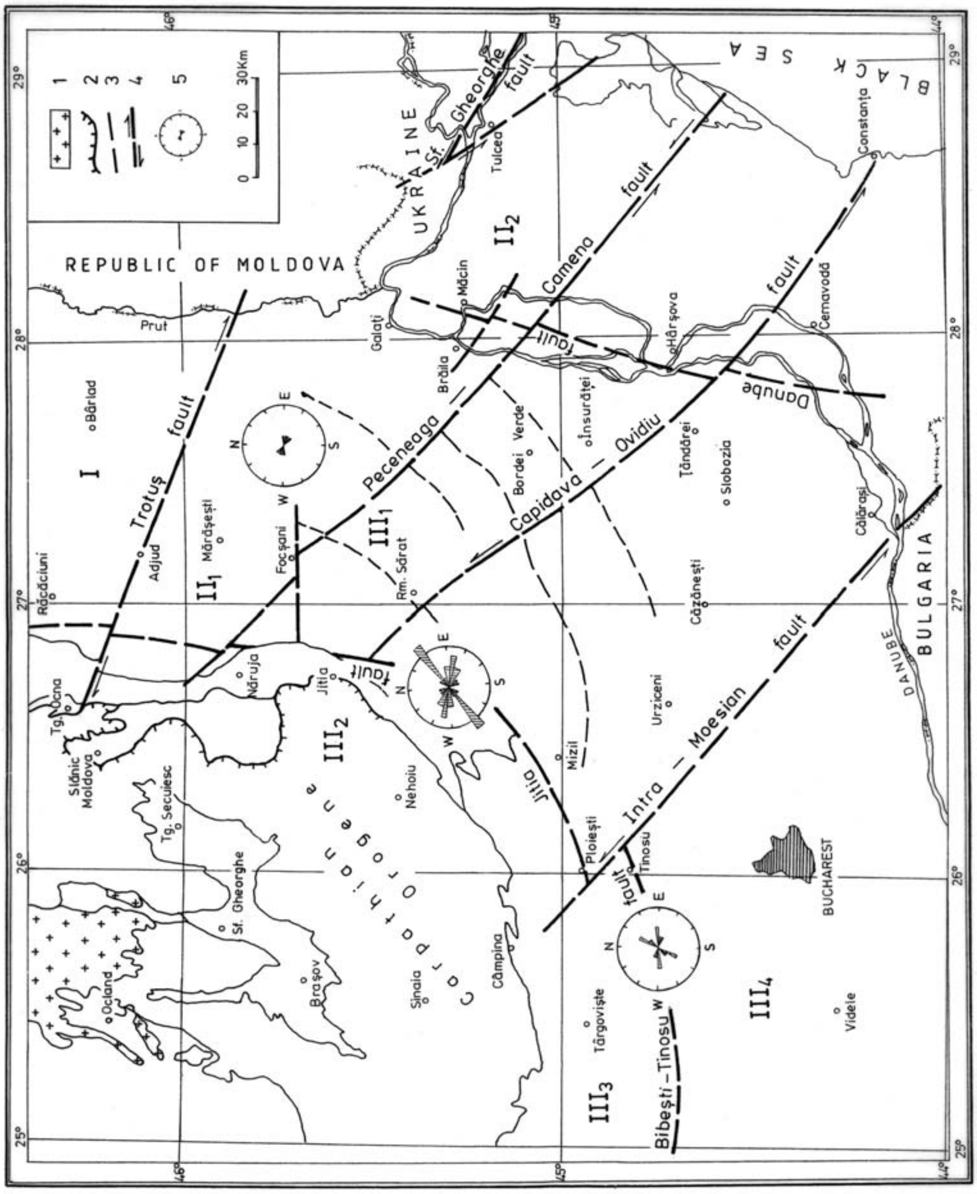

Fig. 2 – Structural simplified map of the Carpathian bend area and the frequency/rose diagrams of the S_{Hmax} azimuths for each tectonic unit. I, Scythian Platform; II_1, North-Dobrujan Promontory; II_2, North Dobrujan Orogen; III, Moesian Platform: III_1, North-Eastern area; III_2, Area covered by the Eastern Carpathians overthrusting; III_3, Area covered by the Southern Carpathians overthrusting; III_4, Central area. 1, Neogene volcanics; 2, Overthrusting line; 3, Crustal fault; 4, Strike-slip fault; 5, Frequency/rose diagram.

Such local change in the orientation of the main horizontal stress is due to the boundary effects associated with geological discontinuities or free surfaces related to the faults, bedding planes, etc. These azimuthal changes can be due, also, to the shape of salt bodies in the diapirs, the principal stresses realigning in the vicinity of the salt diapir structure zone parallel to their margins, the extent of the stress rotation being dependent upon the elastic parameters differences (Goodier, 1933; Schneider, 1985).

Such rotation of the horizontal stress azimuths were documented by: Zoback *et al.* (1989) for the vicinity of the San Andreas fault; Bell (1989) for the faulting along the Scottish Shelf; Shamir and Zoback (1989) in the Cajon Pass, California.

The average orientation of the stress tensors for each compartment, computed by a least squares approach, is presented in Table 2. In the north-eastern sector of the Moesian Platform and in the North Dobrujan Promontory these values are between 110º ± 4º ÷ 112° ± 4°, and in the Orogen covered area -93° ± 6.9°. We have to mention that in our calculation we eliminated the modified azimuths under the influence of local structures.

4. THE PRESENT-DAY STRESS FIELD INFERRED FROM SEISMICITY DATA

4.1. METHODOLOGY

In the study of the seismic source, the focal mechanism expresses the first motion directions of the recorded wave pulses at the stations, determined from the orientations and the direction of slip on the fault. Earthquake focal mechanisms are the only ones which can offer data for the middle to lower crust, from *in situ* measurements, since the fault plane solutions are expressions of the regional stress field and of the way these stresses act at the hypocenter level. Knowing the stress field at the hypocenter level of the crustal earthquakes and the emphasized structure of the upper crust by seismometric data, we can reach a model of the deep active structure.

The P, B, T axes of the earthquake focal mechanisms can be equated, in a simple approach, to the main stress axes σ_1, σ_2 and σ_3. This approximation is available only for a medium of uniform strength. In fact, the medium is inhomogeneous and the slip can occur on preexisting zones of weakness, so that the P, B, T axes from the focal mechanisms are much different from the orientations of the main stress axes.

Among the methods developed to determine the regional stress tensor from a number of earthquake focal mechanism solutions, we applied the methods of Angelier (1984) and Gephart and Forsyth (1984). The latter method assumes that the deviatoric stress tensor is uniform over the region of study and the slip vector of any focal mechanism points to the direction of the maximum solved shear stress of the fault plane (Bott, 1959).

Table 2

Average orientations of the main stress tensors in the geodynamic compartments

Unit				Breakout stress tensors orientations (°)	Seismic stress tensors data					
					σ_1^0	σ_2^0	σ_3^0	R	F	Type of fault
I. Scythian Platform (Southern border)				-	68 ± 8/30	154 ± 4/26	273/61	0,70	4	R
II. North Dobrujan Orogene		Black Sea Block	II_1 N.D.P.	112 ± 4	118/8	206/15	276/28	0,24	10	R
II. North Dobrujan Orogene		Black Sea Block	II_2 N.D.O		130 ± 7,8/30	270 ±5,8/54	40/30	0,78	14	SS, N
III. Moesian Platform	Eastern sector	Black Sea Block	III_1 Focşani Depr.	110,4 ± 4	139 ± 9,2/30	50 ± 8,2/18	270±9,3/70	0,22	14	R, SS
III. Moesian Platform	Eastern sector	Black Sea Block	III_2 Orogene covered area	130,5 ± 3,99	142 ± 11,8/36	238 ± 9,1/6	288 ± 8/78	0,36	18	R, N
III. Moesian Platform	Central Sector		III_3 Orogene covered area	93 ± 6,9	150 ± 9/46	65 ± 7,8/16	282±11/68	0,72	16	R, N
III. Moesian Platform	Central Sector		III_4 Bucharest area		150 ± 9/46	65 ± 7,8/16	282±11/68	0,72	16	R

Kinematic axes $\sigma_1 > \sigma_2 > \sigma$. Stress ratio $R = \frac{\sigma_2 - \sigma_1}{\sigma_3 - \sigma_1}$. Fluctuation (F-average misfit angle); N-normal fault; R-reverse fault; SS- strike-slip fault.

In the inversion scheme, the deviatory part of the stress tensor is represented by four parameters, namely: the orientations of the main stress axes σ_1, σ_2, σ_3 and the shape factor $R = (\sigma_2\text{-}\sigma_{1)} / (\sigma_3\text{-}\sigma_1)$, which specifies the magnitude of σ_2, relative to σ_1 and σ_3 and corresponds to the stress model.

The R value was calculated with the Gephart and Forsyth (1984) method, starting from the two sets of Cartesian coordinates, one fixed by the principal stress directions and the other one fixed by the observed fault plane geometry of the admitted fault.

In the conditions of $\sigma_1 \geq \sigma_2 \geq \sigma_3$ and $0 \leq R \leq 1$, the fault is consistent with the computed stress. The best normative measure of misfit (F), for minimizing the residuals for all observations, is the minimum rotation about any arbitrary axis that brings the fault plane geometry into coincidence with a geometry that satisfies the solution. Two minimum rotation axes for each focal mechanism solution (one for each of the two possible choices for the fault plane) were located. We chose the smallest of the angles as the measure of the misfit, representing the nodal plane which fits the model. To find the model, we adopted the approximate method in a wide ranging grid search (10°). The best stress model was the one with the smallest misfit.

4.2. DATA

In the Carpathian bend area, including the Vrancea region, 72 earthquake focal mechanism solutions were used to solve the orientation of the principal stress axes. The focal mechanism solutions for the crustal events were determined on the P waves first arrival polarities (Enescu, 1963), processed after 1980 with Vickens and Hogart, 1967 Programm (Radu and Oncescu, 1980–1981; Mândrescu *et al.*, 1997).

The quality (Q) of these data, according to the World Stress Map Project (Zoback, 1992; Müller 1993) is expressed by: 2 events of A quality rank (2.7%), 16 events of B quality (22.3%), 48 events of C quality (66.7%) and 6 events of D quality (8.3%).

The seismicity data were used to solve the principal orientations of the stress axes for every event, σ_1, σ_2, σ_3 as well as the shape factor R (Tables 3, 4, 5, 6). We summarize these data in Table 2, which presents the average orientation of stress tensors for each unit (computed by a least squares approach), the shape factor-R, the misfit-F and the main type of faulting for each compartment.

For the interpretation of the stress data we used the lithospheric segmentation presented previously (Zugrăvescu, Polonic, 1997, 2000, 2003), namely the European Plate and the Moesian and Intra-Carpathian Microplates, partially welded in the southern part.

A complete picture of the main horizontal stress tensor variations in relation with the structure features is presented in Fig. 3. In the following, we shall present the mean horizontal stress azimuth for each structural unit in the frame of the plate tectonics of the Romanian territory, as well as the respective type of movement.

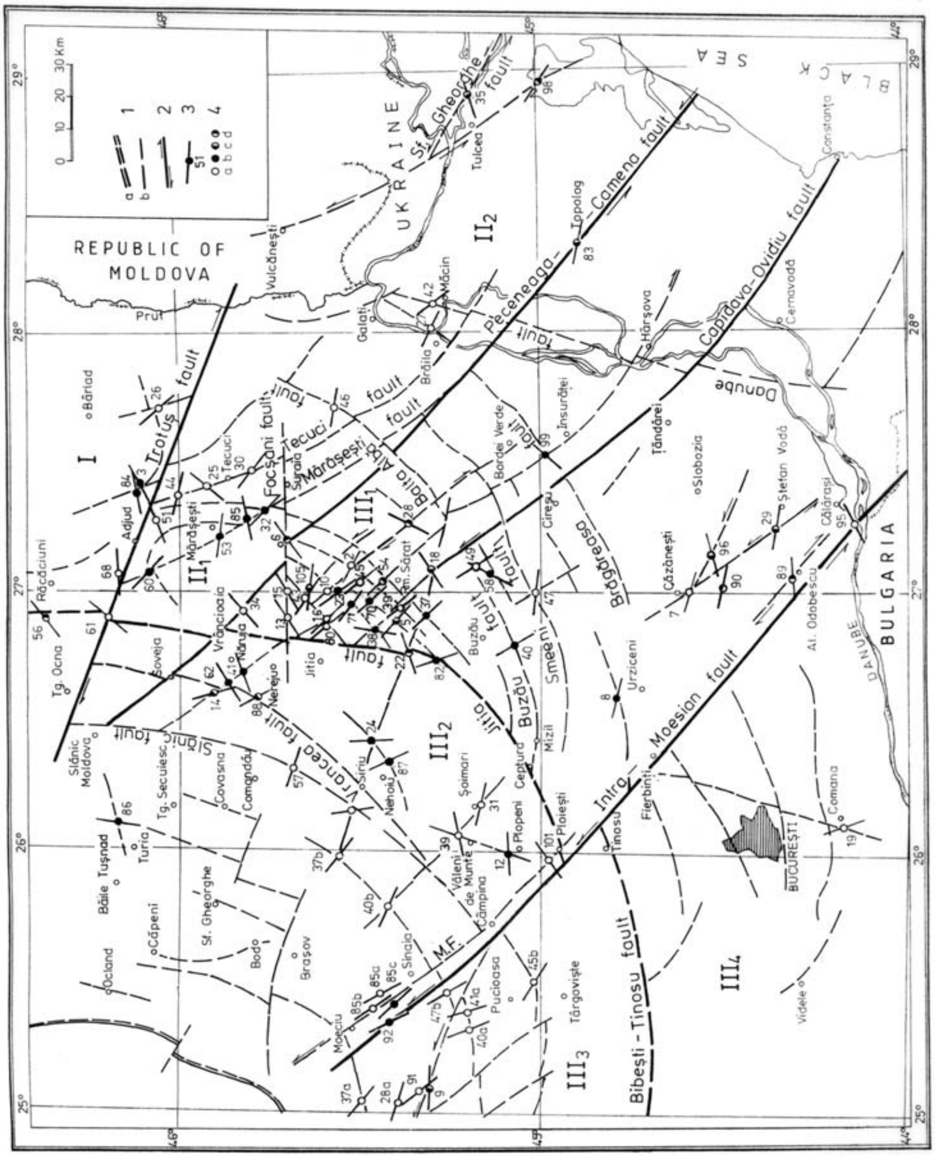

Fig. 3 – The orientation of the main horizontal stress tensors (σ_1) in relation with the deep structure. I, European Plate (Scythian Platform); Moesian Microplate: II_1, North Dobrujan Promontory; II_2, North Dobrujan Orogen; III, Moesian Platform: III_1, North-eastern area; III_2, Area covered by the Eastern Carpathians overthrusting; III_3, Area covered by the Southern Carpathians overthrusting; III_4, Central area. 1, Crustal fault separating the foreland basement in east and the Alpine regenerated basement in west; 2, Crustal fault; 3, Fault; 4, Strike-slip fault; 5, Hypocenter with the focal mechanism solution (no. of event) and the main stress tensor orientation; 6, Type of movement: a – normal; b – reverse; c – senestral strike-slip; d – dextral strike-slip.

On the border of the **European Plate** (I, Fig. 3), the southern part of the Scythian Platform, the few data regarding the maximum horizontal tensors (σ_1) linked to a reverse faulting process, being oriented almost NE-SW (Table 2).

The Moesian Microplate occupies the major part of the studied area, by its north-eastern part, ***the Black Sea Block (BSB)***, limited by two transcurrent faults: the Intra-Moesian one in the west with senestral strike-slip translations and the Trotuş dextral strike-slip fault in the north-east. It is composed of the North Dobruja Orogen (NDO), a folded Alpine area, with its north-western prolongation, the North Dobruja Promontory (NDP), framed within the Carpathian foreland since the Cretaceous, and the eastern sector of the Moesian Platform (MP), with an epi-Paleozoic basement, outcropping in Central Dobruja.

In the BSB, the distribution of the stress data is not uniform. The great density of data appears in the north-western part of the NDP and in the north-eastern sector of the MP.

The North Dobrujan Orogen, *NDO,* (II_2, Fig. 3) presents an orientation of the main principal tensor σ_1=130°/30°, the type of movement being of strike-slip (Table 2).

To the west of the Danube, the structure is dominated by the sinking towards the west and south-west along the Mărăşeşti and Tecuci faults, as well as along the faults which are bordering the NDP (II_1, Fig. 3), taking part in the formation of the northern edge of the Focşani Depression. The type of movement in the Promontory is a composite one, a reverse faulting (Table 2), with a σ_3 stress tensor inclination (28°) bigger than that of the σ_1 stress tensor one (8º), and a normal one with a σ_1 stress tensor inclination (54º) bigger than that of the σ_1 one (30º).

The north-eastern sector of the Moesian Platform (III_1, Fig. 3) concentrates the major part of the seismic derived stress data. They are disposed along the longitudinal faults in its descending part, under the Focşani Depression (N Buzău-Focşani-Jitia area). The orientations of the stress tensors are disposed on a prevailing NW–SE direction with the mean value of σ_1 = 139º ± 9.2/30º, nearly perpendicular to the faults one. The type of movement is, generally, compressive (Table 2), with the σ_3 stress tensor quasi vertical (70º) and the σ_1 stress tensor with a small angle inclination (30º).

In the eastern part, on the Buzău, Smeeni, Brăgăreasa latitudinal faults, the stress tensor orientations present significant misfits regarding the mean value. The cause can be, on the one hand, the location of these seismic stress data at the intersection between the longitudinal fault system with the less extensive transversal one, or, on the other hand, the fact that the principal stress tensors are poorly constrained by few fault plane solutions.

In the western part of the BSB, the IMF with the two main ramifications towards the north, in the area covered by the Orogen (III_2, Fig. 3) displays a prevailing senestral strike-slip movement in regard with the neighbouring Central Moesian Block.

In the sector overthrusted by the Orogen (III_{2-3}, Fig. 3) the seismic derived stress data are restricted and related to the transversal faulting. The mean stress tensor direction is 142º ± 11.8º/36º (Table 2), with a rotation of 3º–5º regarding the eastern compartment III_1, the prevailing type of movement being the reverse one, with a quasi vertical σ_3 mean stress tensor (78º) and a low inclined σ_1 mean one (36º).

As we noticed before (Zugrăvescu, Polonic, 2003), in the III_{1-2} sectors of the BSB, the extensional earthquakes situated in the lower part of the crust display the same stress tensor orientations as those from the NDP. This observation can sustain the prolongation of the NDP under the MP, as already mentioned before by Băncilă (1958) and Mureşan (1971).

The mean stress tensor for the BSB is σ_1 = 137º/32º, meaning the orientation of the compression. As regards the sense of compression, this is towards NW, taking into consideration the dominantly senestral strike-slip movement, the geological offset of the new fractures in the same directions as compared to the neighbouring compartments. The sense of compression is sustained by geodetic data too, which determined horizontal displacements to NW with velocities up to 1.85 mm/year in the north-eastern sector of the IM fault (Nacu *et al.*, 1993).

The Central Moesian sector displays the main stress tensor orientation σ_1 = 150º/46º, which is similar for the both parts of this compartment, covered or uncovered by the Orogen (Table 2 and Fig. 3). In relation with the BSB, the stress orientation is clockwise rotated towards the south by 8–11º. As regards the type of movement, it is of the reverse type, according to the focal mechanism solutions and the greater inclination of the σ_3 stress tensor, in relation with that of σ_1.

The characteristics of the stress field pattern for each crustal compartment came out very clear from the frequency/rose diagrams carried out on the main stress tensors and plotted on the structural simplified map of the Carpathians bending area (Fig. 4). Starting from an obvious WNW–ESE stress azimuth trend for the NDP (118°/8°), the stress orientation shows a clockwise rotation, up to 150º ± 9º/46° for the III_3-III_4 blocks of the MP Central sector. The secondary NE-SW stress orientation is preserved for the III_{1-2} Moesian blocks, but with a low frequency.

5. THE CHANGE OF THE STRESS REGIME WITH DEPTH

To understand the variation of the stress field pattern in depth, we shall consider two aspects: the change of the type of movement as well as of the stress tensor orientation related to the main discontinuities, from the surface towards the base of the crust, namely to the crystalline basement, up to the Conrad and Moho levels.

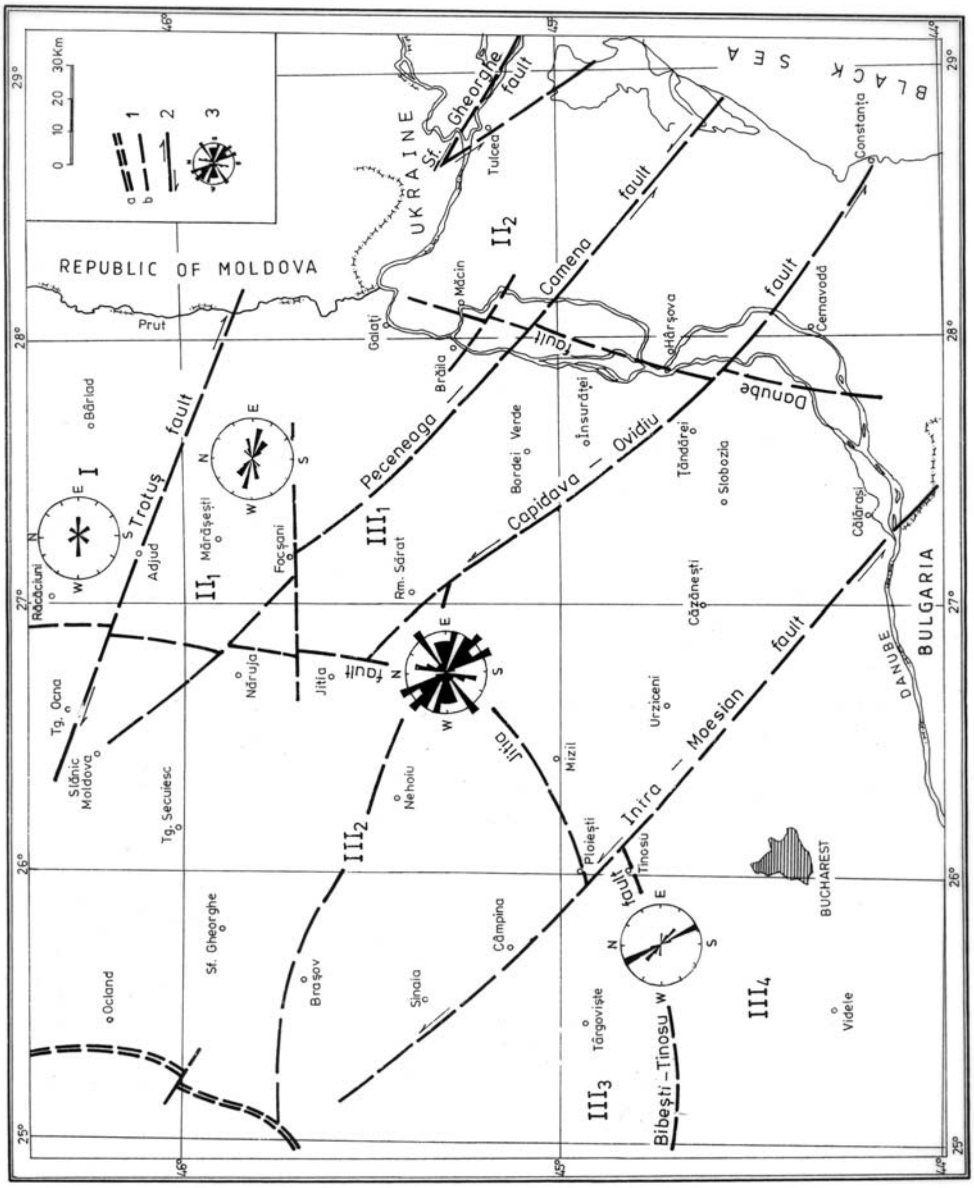

Fig. 4 – Structural simplified map of the studied area and the frequency/rose diagrams of the main horizontal stress azimuths (σ_1) from seismic data, for each crustal compartment. 1: a, Crustal fault separating the foreland basement in the east and the Alpine basement in the west; b, Crustal fault; 2, Strike-slip fault; 3, Frequency/rose diagram for the crustal compartments; For the compartments: I, II, III see Fig. 3.

If we divide the described data of the seismic stress tensor determinations according to the prevalent type of movement associated with a certain depth, we obtain three characteristic sets: one between the depth of 0–15 km; another between 15–30 km and the deepest one between 30–50 km.

The first set comprises the data coming from the sedimentary cover as far as the crystalline basement level, between 0–15 km depth and is characterized by the prevailing strike-slip movement (from 33 stress data 13 are of the strike-slip regime, namely 39.4% and 9 are of the reverse type, 30%).

The second set includes the stress tensor data originated from the seismic events produced between the crystalline basement level and the Conrad discontinuity depths (15–30 km) and reveals a predominant reverse type of the tectonic regime (10 data from a total of 20 focal mechanism determinations, meaning 50%).

The third set is coming from the lower part of the crust, between 30–50 km depth, as far as the Moho discontinuity, where the extensional regime is obvious, representing 58% from the total determinations (11 stress data characterized by normal tectonic movement from a total of 19 data) The characteristics of the three set data enable us to draw the specific stress images at the main crustal discontinuities.

5.1. THE STRESS IMAGE IN THE SEDIMENTARY COVER

In the upper sedimentary cover, up to 5 km, the rose diagrams carried out on the basis of the maximum horizontal stress tensors from the breakout measurements (Fig. 2) show for the NDP (II_1), the two blocks of the Moesian Platform (the north-eastern and the central blocks) a prevalent WNW–ESE orientation of the stress tensors (95–105º), the mean value being 112 ± 4º (Table 2). A secondary orientation, NE–SW observed in the two blocks of the MP covered by the Orogen ($III_{2\text{-}3}$, Fig. 2), can be related to the deviatory effects of the curved fractures from the Orogen nappes, the diapir zone or the foreland units.

The study of the deeper part of the sedimentary cover is based, mainly, on a subset of 11 stress seismic data coming from the deep deposits of the Marginal Folds Nappe and Subcarpathian Nappe units and from the sedimentary cover of the foreland units (Table 3).

The deepest data resulted from the SE Siriu–Nehoiu area, the seismic events having the hypocenters at 9 and 11 km, situated at the base of the Subcarpathian Nappe (events 24 and 87, Table 3) and in the Mesozoic (Jurassic-Cretaceous) deposits of the Moesian Platform cover, under the Focşani Depression (event 43, Table 3). The type of movement seems to be strike-slip and the prevalent azimuths of the main horizontal stress tensors are NNW–SSE in the Orogen covered area and WNW–ESE in the Mesozoic cover of the Moesian Platform.

The image of the stress regime in the upper part of the sedimentary cover in relation with the structure is illustrated by the special map (Fig. 1) and by the frequency/rose diagrams carried out on the basis of the borehole stress data (Fig. 2, 5a) and seismicity stress data (Fig. 5b). From the two main trends displayed in Fig. 5a, the WNW–ESE orientation corresponds to the present-day compressions and displacements, the NE–SW one being parallel to the front of the Carpathians.

Table 3

Stress tensor orientations in the deep sedimentary cover, from the seismicity data

No. event	Date	Time	h/km	M	Rupture plane (°)	σ_1 (°)	σ_2 (°)	σ_3 (°)	R	Fault type	Rank data
22	1980 05 08	01:31:27	5	4.3	015/41	247/38	102/45	330/56	0.49	ss-s	C
24	1980 06 15	06:20:39	11	4.2	310/61	002/00	093/45	274/43	0.58	r	C
31	1980 12 13	19:21:01	4	3.3	010/86	095/44	188/20	284/48	0.49	n-ds	C
37a	1983 03 16	07:58:52	4	3.2	053/89	124/54	202/04	306/65	0.55	n	C
43	1985 06 26	19:11	10	3.3	201/83	097/54	205/24	294/42	0.54	n-ds	C
49	1989 02 26	02:50	4	3.5	051/79	284/53	060/28	147/62	0.56	ss-d	C
54	1990 05 30	23:52	5	3.8	278/90	140/60	278/36	050/48	0.50	ss-d	C
85	1992 10 20	00:50	11	3.0	324/51	258/04	330/70	120/84	0.40	r	C
85a	1993 05 07	11:47:06	6.3	4.1	163/53	113/68	310/48	228/03	0.52	r	B
87	1993 07 21	13:09	9	3.0	241/64	332/40	245/07	106/76	0.24	r	C
91	1994 4 08	15:07:10	4	2.8	074/82	309/70	075/04	137/78	0.52	n	C

Table 4

Stress tensor orientations at the crystalline basement level, from the seismicity data

No. event	Date	Time	h/km	M	Rupture plane (o)	σ_1 (°)	σ_2 (°)	σ_3 (°)	R	Fault type	Rank data
18	1977 03 05	00:00:44	10	5.0	107/85	236/26	104/56	324/53	0.45	ss-s	B
23	1980 05 22	03:19:30	14	4.0	258/60	328/22	068/27	247/71	0.32	r	B
26	1980 08 03	04:11:07	8	3.1	075/33	315/70	076/06	136/82	0.46	n-ds	C
28	1980 10 15	01:55;18	10	3.5	323/89	026/60	117/66	270/24	0.49	ss-d	C
28a	1980 12 04	10:29:59	10	3.7	061/27	274/41	148/54	058/49	0.35	n	C
30	1980 12 11	22:46:31	6	3.2	070/90	135/47	070/12	308/45	0.51	n	C
34	1981 03 05	15:25:	8	2.4	103/87	225/72	103/02	049/83	0.44	n-ds	D
36	1982 06 23	15:51	15	2.4	286/59	012/75	096/20	261/68	0.72	r	D
37b	1983 04 09	00:16:15	7	3.0	135/04	308/60	236/04	124/58	0.12	n	C
41	1984 09 22	23:32	12	3.3	152/56	250/08	157/52	069/85	0.27	r	C
44	1985 07 08	13:25	5	3.5	110/43	093/60	258/29	348/35	0.60	n	C
56	1990 07 19	04:07	10	3.8	187/84	056/53	238/80	314/28	0.50	ss-s	C
57	1990 07 30	12:32	13	2.8	061/39	040/20	127/52	288/50	0.81	n-ds	C
61	1991 07 11	00:41	14	3.0	158/82	032/48	117/86	290/16	0.49	ss-d	C
62	1991 07 12	10:01	8	2.6	157/77	237/37	327/36	092/55	0.32	r	C
83	1992 06 03	20:21	7	3.2	136/55	104/36	262/50	016/78	0.46	ss-s	C
85	1992 10 20	00:50	11	3.0	324/51	258/04	330/70	120/84	0.40	r	C
85b	1993 05 23	17:19:22	8.8	5.1	323/29	266/16	027/80	118/73	0.45	ss-s	A
85c	1993 05 23	19:24:12	7.9	4.3	198/65	078/46	234/54	320/25	0.35	r	B
96	1994 07 15	09:28:30	4	3.0	121/75	076/48	286/36	202/82	0.55	ss-s	C
98	1994 08 19	14:33:32	4	2.4	158/45	121/50	272/42	031/45	0.53	ss-d	D
105	1997 12 06	12:17:25	16	4.0	057/70	100/48	258/39	346/82	0.45	ss-s	C

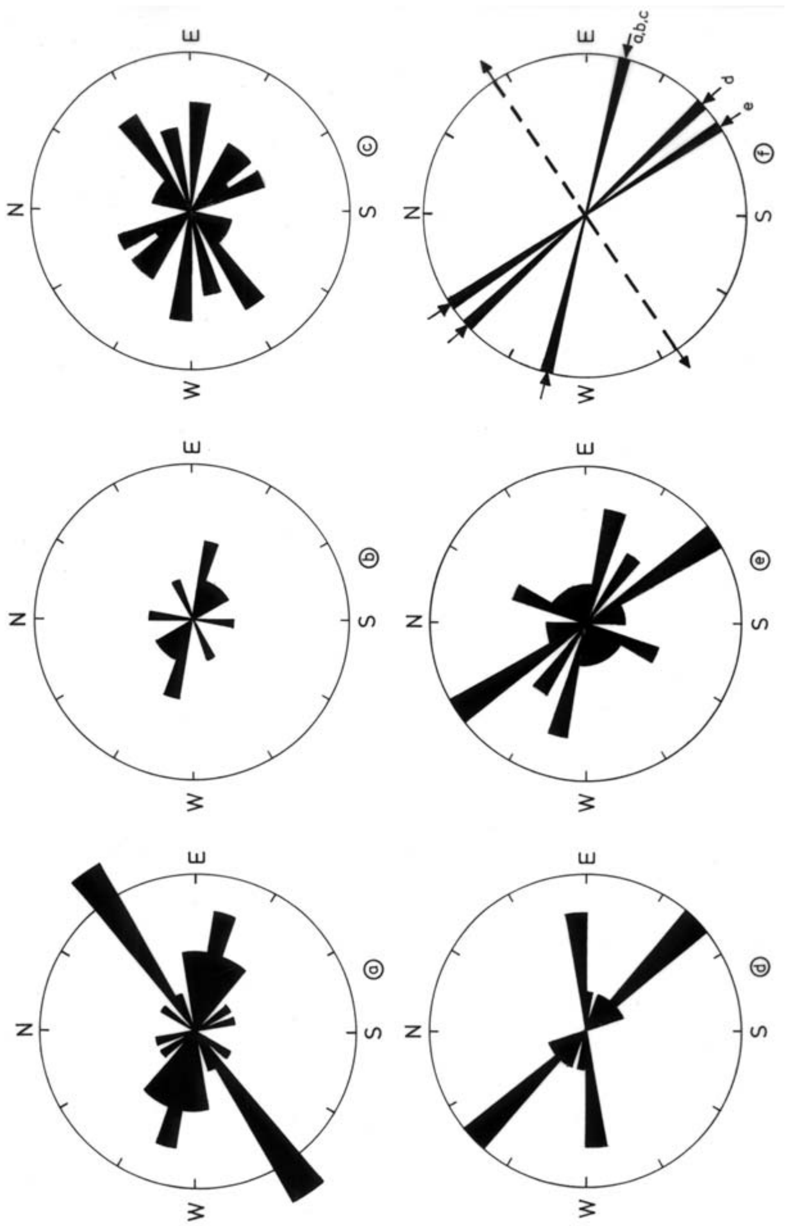

Fig. 5 – Frequency/rose diagrams at different structural levels, based on: a, Stress data determined by the borehole method (S_{Hmax}) in the upper sedimentary cover; b, Seismicity stress data (σ_1) in the lower sedimentary cover; c, Seismicity stress data (σ_1) at the sedimentary cover/crystalline basement boundary; d, Seismicity stress data (σ_1) in the upper crust, up to the Conrad discontinuity; e, Seismicity stress data (σ_1) in the lower crust, up to the Moho discontinuity; f, Variation of the mean stress tensor orientations into the crust, at the levels mentioned above.

5.2. THE STRESS IMAGE AT THE CRYSTALLINE BASEMENT LEVEL

As the contrast between the elastic properties of the crystalline basement and the overlying sediments can produce some changes in the stress orientation (Bell and Lloyd, 1989), we paid a special attention to the stress image at this level. To obtain this image, we correlated the seismicity information (coordinates, depth, magnitude, seismic stress data) with the crystalline basement structure (Polonic, 1996, 1998, 2002). The hypocenters of the crustal events are disposed, generally, at the intersection of the crystalline basement level with the major crustal faults, like: Mărăşeşti, Tecuci, Slănic faults (Zugrăvescu, Polonic, 2003).

Though the seismic stress data give a rather dispersed orientation of the stress tensor, a predominant trend of a WNW–ESE stress orientation could be detected (Fig. 5c).

The data subset comprising a number of 22 stress azimuth determinations, from the first set mentioned above, reveals as a prevalent type of movement the strike-slip one (41% from the total of data, see Table 4).

5.3. THE STRESS IMAGE AT THE CONRAD DISCONTINUITY

A set of 20 stress data is coming from the hypocenters disposed along the Conrad discontinuity, at the intersection with transcrustal faults, as: Mărăşeşti, Tecuci, Balta Albă a.o. faults (Fig. 3). The stress tensor orientations show a bimodal distribution: a dominant NW–SE trend and a subsidiary ENE–WSW one (Fig. 5d). The predominant type of movements seems to be the reverse one (50%, 10 determinations from the total of 20 measurements, Table 5).

5.4. THE STRESS IMAGE IN THE LOWER PART OF THE CRUST

The set of 19 stress determinations, selected for the lower part of the crust, shows an obvious normal type of movement (11 determinations from the total of database, meaning 58% (Table 6). The azimuth frequency/stress diagram built on the basis of the stress orientations shows a symmetrical dispersed data against a dominant and consistently NW-SE oriented axes (Fig. 5e).

From the analysis of the stress tensor orientations in depth, related to the main tectonic discontinuities, we observe the following (Fig. 5):

– in the sedimentary cover, at a first step of depth up to 5 km, the azimuth frequency/rose diagram show a prevalent WNW–ESE orientation of the stress tensors determined with the breakouts method, as well as a secondary deviatory trend, NE–SW explained above (Fig. 5a);

– in the deepest deposits of the sedimentary cover up to about 10 km depth (Fig. 5b), the stress tensors derived from seismicity data expose the same dominant WNW–ESE orientation (about 105º), which rests as a homogeneous zone, the secondary deviatory trend NE-SW being preserved, but with a low frequency;

Table 5

Stress tensors orientations at the Conrad discontinuity level, from the seismicity data

No. event	Date	Time	h/km	M	Rupture plane (°)	σ_1 (°)	σ_2 (°)	σ_3 (°)	R	Fault type	Rank data
1	1952 06 03	05:35:25	20	5.0	359/84	094/38	006/82	263/52	0.52	n	B
3	1956 04 18	12:52;26	20	4.5	338/77	262/44	150/38	060/51	0.48	r	B
5	1957 12 23	23:38:45	25	4.0	030/80	132/50	043/37	277/42	0.60	ss-s	C
12	1975 02 08	08:21:18	23	4.7	343/80	085/35	340/92	250/58	0.49	r	B
14	1975 03 07	04:13:05	21	5.1	030/88	159/24	079/80	255/14	0.45	ss-s	B
19	1977 04 20	21:16:00	11	3.9	190/80	288/40	070/50	160/50	0.48	r	C
25	1980 06 16	18:43:30	22	4.5	068/22	040/54	125/24	257/55	0.43	n-ds	B
27	1980 09 11	23:24:26	12	4.7	052/87	129/65	053/12	297/52	0.51	n-ds	B
29	1980 12 08	19:51:17	15	3.8	331/85	277/33	129/61	039/68	0.41	ss-s	C
32	1981 02 16	23:27	24	3.3	078/83	136/68	257/06	049/88	0.45	r	C
37	1983 02 21	18:03:56	19	4.7	234/63	312/19	047/23	248/88	0.47	r	C
39	1983 05 23	22:35:06	20	2.9	340/89	074/50	161/08	259/44	0.54	n-ds	C
46	1987 08 19	02:18	21	4.2	029/48	074/88	201/48	104/04	0.78	n	C
47	1988 02 20	01:06:	26	3.3	335/44	122/86	032/70	276/12	0.64	n	C
51	1989 12 28	22:22:	22	3.5	330/80	250/58	330/02	067/39	0.61	n-ds	C
60	1990 10 11	10:51:	22	4.3	066/54	136/09	233/26	070/78	0.31	r	B
70	1991 08 31	22:43:	24	3.2	040/76	138/46	048/27	277/54	0.42	r	C
80	1992 01 28	14:35:	24	2.5	019/39	320/28	066/32	240/70	0.40	r	C
86	1993 07 01	15:08:	19	2.3	078/48	006/35	096/20	270/68	0.23	r	D
99	1994 09 16	14:03:18	21	2.3	295/73	040/41	298/12	242/87	0.44	r	D

Table 6

Stress tensor orientations at the Moho discontinuity, from the seismicity data

No. event	Date	Time	h/km	M	Rupture plane (°)	σ_1 (°)	σ_2 (°)	σ_3 (°)	R	Fault type	Rank data
2	1954 10 01	13:31:10	50	5.2	037/76	000/70	216/25	123/14	0.72	n	A
7	1960 01 04	12:51:52	41	5.4	137/39	109/74	285/24	026/29	0.57	n	B
8	1967 02 27	21:00:43	46	5.0	021/40	282/11	194/44	082/78	0.16	r	B
10	1969 12 21	19:06:23	33	4.6	050/78	140/55	054/18	331/61	0.39	n-ds	B
13	1975 03 02	13:21:00	40	4.1	276/86	322/74	094/20	233/66	0.42	n	B
16	1975 05 26	22:04:00	50	4.1	106/89	319/81	104/26	233/52	0.16	ss-d	C
40	1984 06 05	14:36:	37	3.3	052/59	148/28	059/11	277/75	0.20	r	C
40a	1983 11 14	16:22:	48	2.6	283/35	276/60	057/26	158/48	0.75	n	C
41a	1985 02 01	06:35:	50	2.8	268/49	264/73	073/18	342/10	0.70	n	C
45b	1986 12 02	22:44:	31	3.5	238/84	120/68	238/09	314/58	0.72	n	C
47	1988 02 20	01:06	26	3.3	335/44	122/86	032/70	276/12	0.64	n	C
47b	1988 03 12	23:10:	50	3.3	098/86	332/30	088/37	217/53	0.75	n	C
53	1990 04 06	12:35:	37	2 4	200/40	101/08	014/50	260/80	0.81	r	D
58	1990 09 29	05:06:	34	2.8	112/70	208/61	104/05	064/88	0.29	r	C
71	1991 09 01	01:15:12	32	4.8	105/61	206/25	297/31	091/61	0.25	r	B
82	1992 03 03	14:18:	36	2.8	247/51	343/20	254/08	094/83	0.11	r	C
84	1992 08 29	12:38:	37	2.8	003/56	076/13	158/60	285/72	0.34	r	C
95	1994 05 30	13:07:49	40	2.5	132/83	051/72	132/20	243/43	0.54	n-ds	C
100	1994 09 29	21:29:24	46	3.0	279/57	259/80	095/09	011/80	0.91	n	C

– from the crystalline basement level towards depth, we observe a gradual clockwise rotation of the seismic stress tensor orientations, namely from 125º at this level (Fig. 5c), to 135º at the Conrad discontinuity (Fig. 5d), up to 155º at the Moho discontinuity (Fig. 5e). A synthesis of the clockwise rotation of the main stress tensor orientations is plotted in Fig. 5f.

As regards the tectonic regime, the change of the movement type with depth may be determined by two factors:

– the increase of the horizontal stress in the upper part of the crust, due to the continental collision from the Vrancea region, expressed by the prevalence of the compressive regime, and

– the increase of the vertical stress in the lower crust, due to the increase of the lithostatic weight, expressed by an extensive regime.

The geodynamic model proposed for the Vrancea region (Polonic, 1996; Zugrăvescu, Polonic 1997, 2003), based on geological and geophysical data, assumed a NW plunging of the BSB of the Moesian Microplate under the Intra-Carpathian Microplate. In the upper crust, the continental collision of these crustal compartments show a general compression acting from SE, providing an increase of the horizontal stress, materialized by a strike slip movement up to the crystalline basement level and a reverse one at the Conrad discontinuity, by a tectonics of shorting and a underthrusting block tendency.

The SE compression is realized by the processes from the northern part of the Black Sea basin, by the pushing of the Arabian and Anatolian Plates, created by the Red Sea-Aden Bay rift, as well as by the approaching movement of the African Plate towards the Eurasian one, in the frame of an anticlockwise rotation of 10 mm/year velocity (Rebai *et al.*, 1992). This movement towards the north, towards the microplates mosaic between the two major plates, the African and the Eurasian ones, recorded at the GPS stations situated north of the Anatolian fault (Reillinger *et al.*, 1997; Mc Kluski *et al.*, 2000), is transmitted in the BSB of the Moesian Microplate and registered at the Vrâncioaia station (VRAN from the Central European GPS Geodynamic Network – CEGRN), with a NW orientation and a 4 mm/year mean velocity of the horizontal displacement for the 1994–1997 period (Bălă, 2000).

For the lower crust, below the depth of 25–30 km up to the Moho discontinuity (about 50 km), an increase of the lithostatic weight (due also to the overburden masses of the Carpathian nappes), can produce an increase of the deviatory component along the vertical axis. This process creates the change from a compressional tectonic regime in the upper crust to the extensional one in the lower part of the crust.

6. CONCLUSIONS

The paper presents a detailed analysis of the present-day stress field pattern in the Carpathian bend area, determined by the breakouts method and by the inversion method of earthquake focal mechanisms solutions. The analysis was performed using a data set of 37 breakout determinations for the upper part of the sedimentary cover (0–5 km) and 72 reliable fault plane solutions of crustal earthquakes, processed with the inversion methods of Angelier (1984) and Gephart and Forsyth (1984), for the entire thickness of the crust.

The regional stress field in the Carpathian bend area has a homogeneous character expressed by the prevalence of a NW–SE orientation of the main stress tensors in the Moesian Microplate (Fig. 3), with a clockwise rotation of about 30°, in the horizontal plane (Fig. 4), between the NDP (mean value 118º, Table 2), the BSB of the MP (mean value 137°) and the Central Block of the MP (mean value 150 ± 9°).

As regards the northern border of the region, belonging to the Scythian Platform (European Plate), the few seismic stress tensors reveal a NE–SW orientation (68° ± 8°).

The intra-plate stress field from the Carpathian bend area, controlled by the continental collision and by the compressional forces applied at the plate boundaries, with a NW-SE prevailing orientation, can be considered of the “first order” (in the meaning of Zoback, 1992). Superimposed on this “first order” regional stress field, there is a second order stress field, NE–SW oriented, due to the local anomalies, which are disturbing the regional one. In the studied area, these local anomalies are of a tectonic origin, such as: the presence of the free surfaces related to the faults planes (see the crustal IMF as well as the longitudinal faults), boundary effects associated with geological discontinuities, salt diapir structure a.s.o. The interference between the regional and local stress fields generates, in the Carpathian bend area, the right angle clockwise rotation of the main stress tensors, between the NDP, north-eastern and central blocks of the MP.

It is obvious that the tectonic regime is a compressional one, the reverse type of movement being characteristic for the European Plate border and some tectonic units from the Moesian Microplate (NDP, the western part of the BSB) and the strike-slip movement for the rest of the BSB.

The sense of compression, towards north-west, from the Black Sea Basin, is documented by geological and geophysical evidence: the existence of a N–S compression (on seismic data) in the NW part of the Black Sea Basin, transmitted through the crustal PC and CO faults towards the Carpathian bend area; the reduction close to the disappearence of the outer border of the Subcarpathian Nappe (the Pietricica–Tazlău structure) covered by the western flanc of the Focşani Depression. The backwards orientations of the nappes planes and faults and the appearence, in the front area of the Carpathians, of numerous reverse faults with SW inclinations; the geological offsets of the new fractures, crossing the BSB, in the same NW direction. The geodetic evidence, of small horizontal displacements towards NW, with velocities up to 1.85 mm/year in the north-eastern sector of the IM fault (Nacu *et al.*, 1993) and at Vrâncioaia (VRAN station from the CEGRN), up to 4 mm/year, mean velocity for the 1994–1997 period (Bălă, 2000), sustain this sense of compression.

The reasons for the SE towards NW compression can be the processes from the Black Sea Basin, the pushing of the Arabian and Anatolian Plates, created by the drift of the Red Sea–Aden Bay rift and the general approaching movement of the African Plate towards the Eurasian Plate, with a 10 mm/year mean velocity (Rebai *et al.*, 1992).

The study of the stress field variation in depth revealed two aspects: the change of the stress orientation and of the tectonic regime.

The stress field pattern has an almost constant orientation in the sedimentary cover (105°), determined by the both used methods, breakouts and inversion of seismic data (Fig. 5a, 5b). From the crystalline basement level towards depth, the seismic stress tensor orientations show a gradual clockwise rotation, from 125° at this level (Fig. 5c) to 135° at the Conrad discontinuity (Fig. 5d) up to 155° at the Moho discontinuity (Fig. 5e).

The change of the tectonic regime with depth is determined by two factors:

– the increase of the horizontal stress in the upper part of the crust, due to the continental collision of the crustal compartments, in the general compression acting from SE, expressed by the prevalence of the compressive regime and materialized by a strike-slip regime up to the crystalline basement level and a reverse one up to the Conrad discontinuity, by a tectonics of shortening and an underthrusting block tendency;

– the presence of the vertical stress in the lower crust, up to the Moho discontinuity, due to the increase in the lithostatic pressure, materialized by an extensive regime.

Acknowledgements. The present study was carried out with the support of the Institute of Geodynamics, Themes IG-1.7-2003-2004.

REFERENCES

ANDERSON, E.M. (1951), *The dynamics of faulting and dyke formation, with application in Britain*, 2nd Edition. Oliver and Boyd, Edinburgh.

ANGELIER, J. (1984), *Tectonic analysis of fault slip data.* J. Geophys. Res., **89, B7,** 5835–5848.

BĂLĂ, A. (2000), *Contributions to the knowledge of the structure and dynamics of the lithosphere. Application in some areas of Romania* (in Romanian), Ph. D. Thesis, pp. 220.

BĂNCILĂ, I. (1958), *The geology of the Eastern Carpathians* (in Romanian). Ed. Ştiinţifică, pp. 367.

BELL, J.S. (1990), *Investigating stress regimes in sedimentary basins using information from oil industry wireling logs and drilling records.* Geol. Soc. Spec. Publ., London, **48,** 305–325.

BELL, J.S., LLOYD, P.F. (1989), *Modelling of stress refraction in sediments around the Peace River Arch, Western Canada.* Current. Res., **D, 89-1D,** 49–54.

BOTT, M.H.P. (1959), *The mechanism of oblique slip faulting.* Geol. Mag., **96,** 109–117.

CONSTANTINESCU, L., MÂRZA, V. (1980), *A computer compiled and computer oriented catalogue of Romania's earthquakes during a millennium.* Rev. Roum. Géol., Géophys., Géogr. (Géophysique), **24, 2,** 193–234.

ENESCU, D. (1963), *The focal mechanism of some crustal Carpathian earthquakes.* Com. Acad. Rom. (in Romanian), **XII, 2**, 1291–1299.

GEPHART, J. W., FORSYTH, D. (1984), *An improved method for determining the regional stress using earthquake focal mechanism data: Application to the San Fernando earthquake Sequence.* J. Geophys. Res., **89, B11,** 9305–9320.

GOODIER, J.N. (1933), *Concentration of stress around spherical and cylindrical inclusions and flows*. Trans. Soc. Amer. Mec. Engin., **55**, 39–47.

HAUSER, F., RĂILEANU, V., FIELITZ, W., BĂLĂ, A., PRODEHL, C., POLONIC, G., SCHULZE, A. (2001), *Vrancea-99*, *The crustal structure beneath the South-Eastern Carpathians and the Moesian Platform, from a seismic refraction profile in Romania.* Tectonophysics**, 340,** 233–256.

IONESI, L. (1994), *Geology of the foreland units and of the North Dobrujan Orogen* (in Romanian). Ed. Tehnică, pp. 280.

LANDES, M., FIELITZ, W., HAUSER, F., POPA, M., CALIXTO Group (2004), *3-D, Upper crustal tomographic structure across the Vrancea seismic zone, Romania.*Tectonophysics, **382,** 85–102.

MÂNDRESCU, N., ONCESCU, M.C., POPA, M., UTALE, A. (1997), *The catalogue of focal mechanism solutions.* In: F. Wenzel, D. Lungu and O. Novak (Eds.): *Vrancea Earthquakes: Tectonics, Hazard and Risk Mitigation*. Kluwer Acad. Publish.

MC. CLUSKI, S., BALASSIAN, S., BARKA, A., DEMIR, C., ERGINTAV, S., GEORGIEV, I. (2000), *GPS constraints on plate kinematics and dynamics in the Eastern Mediteranean and Caucasus.* J. Geophys. Res., **105.**

MÜLLER, B. (1993), *Tectonic stress in Europe. Borehole guided waves affected by stress induced anisotropy.* Ph. D. Thesis, University of Karlsruhe.

MUREŞAN, M. (1971), *On the presence of tectonic window in the green schists zone in Dobruja (Altân Tepe region)* (in Romanian). D.S. Inst.Geol., **LVII/5,** 127–154.

NACU,V., RĂDULESCU, F., MATECIUC, D., STIOPOL, D. (1993), *Horizontal deformations parameters in the Gruiu-Căldăruşani geodynamic Polygon in Romania.* Rev. Roum. Géophysique, **87**, 19–28.

NEGUŢ, A., DINU, C., SAVU, I., BARDAN, R., NEGUŢ, M.L., CRAICIU, I. (1994), *Stress orientation determination in Romania by borehole breakouts. Geodynamic significance.* Rev. Roum. Géophysique*,* **38,** 45–56.

NEGUŢ, A., DINU, C., NEGUŢ, M., IVAN, M., NICULESCU, B. (2000), *State of stress orientation determination in Romania by borehole breakouts.* SEG/EAGE/RSG Bucharest Intern. Geophys. Conf.., **1/2000**, 10–14 april, 418–420.

ONCESCU, M.C., MÂRZA, V., RIZESCU, M., POPA, M. (1999), *The Romanian earthquake catalogue between 984–1996.* In: F. Wenzel, D. Lungu, and O. Novak (Eds.): *Vrancea earthquakes: Tectonics, Hazards and Risk Mitigation*. Kluwer Acad. Publish, 43–49.

PARASCHIV, D. (1979), *The Geology of the Romanian Oil and Gas Fields* (in Romanian). St. tehn. ec., **A, 13,** pp. 382.

POLONIC, G. (1996), *Structure of the crystalline basement in Romania.* Rev. Roum. Géophysique, **40,** 57–70.

POLONIC, G. (1998), *The structure and morphology of the crystalline basement in Romania.* CERGOP, South Carpathians Monograph, **7 (37),** 127–131, Warszawa.

POLONIC, G. (2000), *Neogene dynamics of some crustal compartments on the Romanian territory.* Rev. Roum. Géophysique, **44**, 35–56.

POLONIC, G. (2002), *The structural and morphological map of the crystalline basement in the bending area of the Eastern Carpathians.* St. cerc. Geofizică, **40,** 27–37.

RADU, C., ONCESCU, M.C. (1980-1981), *Catalogues of earthquake focal mechanism solutions* (in Romanian). Intern. Rep., I.Ph.E.S.

RĂDULESCU, D.P., CORNEA, I., SĂNDULESCU, M., CONSTANTINESCU, P., RĂDULESCU, F., POMPILIAN, A. (1976), *Structure de la croûte terrestre en Roumanie. Essai d'interprétation des études sismiques profondes.* An. Inst. Geol. Geofiz., **L, 50,** 5–36.

RĂDULESCU, F. (1988), *Seismic models of the crustal structure in Romania.* Rev. roum. géol., géophys., géogr. (Géophysique), **32,** 13–17.

REBAI, S., PHILIP, H., TABOUDA, A. (1992), *Modern tectonic stress field in the Mediterranean region. Evidence for variation in stress directions at different scales.* Geophys. Journ. Inter., **110,** 106–140.

REILLINGER, R.E., MC CLUSKI, S.C., ORAL, M.B., KING, R.W., TOKSOZ, M.N. (1997), *GPS Measurements of present-day crustal movements in the Arabia-Africa-Eurasia Plate collision zone.* J. Geophys. Res., **102, B5,** 9983–9999.

SĂNDULESCU, M. (1984), *Geotectonics of Romania* (in Romanian). Ed. Tehnică, pp. 336.

SĂNDULESCU, M. (1988), *Cenozoic tectonic history of the Carpathians*. In: L.H. Royden, F. Horvath (Eds): *The Pannonian Basin. A study in basin evolution*, AAPG, Memoirs, **45,** 17–25.

SĂNDULESCU, M., VISARION, M. (2000), *Crustal structure and evolution of Carpathian-western Black Sea areas.* First Break, **18,** 103–108.

SCHNEIDER, F. (1985), *Bohrlochrandausbrueche in norddeutschen Bohrungen und ihm Beziechung zum regionalen Spunnungensfeld –Beobachtung und Theorie.* Ph.D. Thesis, University of Karlsruhe.

SHAMIR, G., ZOBACK, N.D. (1989), *The stress orientation profile in the Cajon Pas – California, scientific drillhole based on detailed analysis of stress induced borehole breakouts.* Proc. Rock at Great Depth, Pau, 1041–1948, Rotterdam.

TĂRĂPOANCĂ, M., BERTOTTI, G., MAȚENCO, L., DINU, C., CLOETINGH, S.A.P.L. (2003), *Architecture of the Focşani Depression: a 13 km deep basin in the Carpathian Bend zone (Romania).* Tectonics, **22**, 6, 13_1-13_{17}.

ZOBACK, M.L., ZOBACK, M.D., ADAMS, J., ASSUMPSAO, M., BERGMAN, G.A., BERETON, N.R., FUCHS, K., GREGERSON, S., MÜLLER, B., STEPHANSSON, O. *et al.* (1989), *Global patterns of tectonic stress.* Nature, **341**, 291–298.

ZOBACK, M.L. (1992), *First and second order patterns of stress in the lithosphere. The World Stress Map Project.* J. Geophys. Res., **97,** 11703–11728.

ZUGRĂVESCU, D., POLONIC, G. (1997), *Geodynamic compartments and present-day stress state on the Romanian territory.* Rev. Roum. Géophysique, **41,** 3–24.

ZUGRĂVESCU, D., POLONIC, G. (2000), *Present-day stress field inferred from seismicity data.* XXV Gen. Assemb. EGS, Nice, France, 25–29 April, 2000.

ZUGRĂVESCU, D., POLONIC, G. (2003), *Active tectonic processes, cause of the crustal seismicity in the Vrancea region.* Rev. Roum. Géophysique, **46,** pp. 3–30.

ZUGRĂVESCU, D., POLONIC, G., NEGOIȚĂ V.(1998), *Determination of stress orientations by geophysical methods on the Romanian territory* (in Romanian). Bul. I.G.A.R, **9/1**, 2–47.

ZUGRĂVESCU, D., POLONIC, G., NEGOIȚĂ, V. (2000a), *Borehole measurements inferred in a high seismic risk zone.* Rev. Roum. Géophysique, **44,** 87–97.

ZUGRĂVESCU, D., POLONIC, G., NEGOIȚĂ, V. (2000b*), Stress and pressure regime in the Căldăruşani–Tulnici Geodynamic Polygon (depth interval 5,000–7,000 m).* SEG/EAGE/RSG Bucharest Intern. Geophys. Conf., 10–14 April, **1/2000,** 344–345.

ZUGRĂVESCU, D., POLONIC, G., NEGOIȚĂ, V. (2002), *Using well logs for geodynamic processes knowledge. Application in the Vrancea zone – Romania.* Bul. Univ. Petrol, Ploieşti, **LIV,** seria Tehnică, **9,** 250.

Received: October 4, 2004
Accepted for publication: October 27, 2005